JPE 7-1-8

A Novel Active Anti-islanding Method for Grid-connected Photovoltaic Inverter

Youngseok Jung*, Jaeho Choi†, and Gwonjong Yu*

*School of Electrical and Computer Eng., Chungbuk National University, Cheongju, Korea
**Photovoltaic Research Group, Korea Institute of Energy research, Daejeon, Korea

ABSTRACT

This paper proposes a novel active frequency drift (AFD) method to improve the islanding detection performance with minimum current harmonics. To detect the islanding phenomenon of grid-connected photovoltaic (PV) inverters concerning the safety hazards and possible damage to other electric equipment, anti-islanding methods have been described. The AFD method that uses chopping fraction (*cf*) enables the islanding detection to drift up (or down) the frequency of the voltage during the islanding situation. However, the performance of the conventional AFD method is inefficient and causes difficulty in designing the appropriate *cf* value to meet the limit of harmonics.

In this paper, the periodic chopping fraction based on a novel AFD method is proposed. This proposed method shows the analytical design value of *cf* to meet the test procedure of IEEE Std. 929-2000 with power quality and islanding detection time. To verify the validation of the proposed method, the islanding test results are presented. It is confirmed that the proposed method has not only less harmonic distortion but also better performance of islanding detection compared with the conventional AFD method.

Keywords: islanding, grid-connected PV systems, active frequency drift method, non-detection zone

1. Introduction

An important requirement for the connection of the photovoltaic (PV) system to the distribution networks is the capability of islanding detection. Islanding occurs when a portion of the distribution system becomes electrically isolated from the remainder of the power system, yet continues to be energized by the grid-connected PV system. Failure to trip the PV system during the islanding situation can lead to a number of problems to the PV system and connected loads. Therefore, both utility companies and applicable standards require the PV systems to include an islanding prevention function [1].

Passive anti-islanding schemes rely on the detection of certain distinct patterns or signatures at the PV system output when islanding occurs. However, there is a relatively large non-detection-zone (NDZ); therefore it is common for the standard protection relays (under/over voltage relay and under/over frequency relay) to use basic protection schemes while other passive methods (e.g.

Manuscript received May. 15, 2006; revised Dec. 13, 2006
†Corresponding Author: choi@chungbuk.ac.kr
Tel: +82-43-261-2425, Fax: +82-43-276-7217,
Chungbuk Nat'l Univ.
*School of Electrical and Computer Eng., Chungbuk Nat'l Univ.
**Photovoltaic research group, Korea Institute of Energy Research

phase jump detection) are used as secondary protection schemes [2].

In active anti-islanding schemes, the perturbation uses active signal injection into the PV system output. The power balance between the PV system and local loads when the islanding occurs can be broken with this perturbation, so active methods are generally considered more effective than passive ones [2]. However the power quality or output power generation is impaired by this perturbation due to the change of magnitude or frequency of the output voltage or current. Therefore, it is necessary to consider the restriction standard concerned with power quality and islanding detection time. Among the active islanding methods, the active frequency drift method (AFD) has received recent attention[3]. AFD is implemented by adding a short period of zero time into the output current of the inverter, as shown Fig. 1.

The ratio of the zero time T_z, to half of the period of the voltage waveform, T_{grid}, is referred to as the "chopping fraction" (*cf*):

$$cf = T_z / T_{grid} \tag{1}$$

The chopping fraction enables the islanding detection to drift up (or down) the frequency of the voltage in the islanding situation. But due to the fixed value of *cf*, the conventional AFD has a large NDZ and is too slow to meet the islanding detection time limit. An active frequency drift with positive feedback (AFDPF) method has been developed to change the *cf* with the positive feedback as shown in Eq. (1) [4]:

$$cf_k = cf_{k-1} + F(\Delta\omega_k) \tag{2}$$

AFDPF method offers significant improvement over AFD by preventing "leveling off" of the frequency until much larger frequency errors are attained. The primary design issue of AFDPF is how to sway the frequency quickly from the nominal value during islanding [2]. Ultimately, it was not clearly described in previous research. A systematic approach to design the feedback gains of AFDPF (as it is called SFS: Sandia frequency shift) was presented in [5]. However, there is no mention about the relation between the feedback gains and power quality limit.

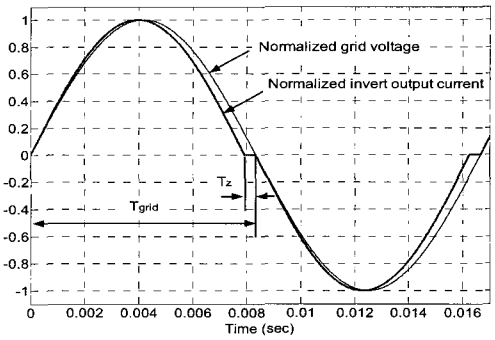

Fig. 1 Example of a waveform using AFD.

In this paper, a novel AFD method with a pulsation of chopping fraction is proposed. It describes how to design the value and the variation period of *cf* to meet IEEE Std. 929-2000 with the power quality and islanding detection time limits. To verify the validation of the proposed method, the islanding test results are presented for a single-phase PV system. It is verified that the islanding can be detected in 2 seconds with less than 5% *THDi*, which is recommended in the mentioned standard [9].

2. Synopsis of IEEE Std. 929-2000

This standard is focused on providing the recommended practice for utility interconnection of PV systems and the islanding test procedure. It is shortly described as the following:

1) Power quality: The total harmonic distortion of current (THD_i) should be less than 5% of the fundamental frequency current at rated inverter output and each individual harmonic should be below the limits listed in Table 1. The PV system should operate at the power factor (*pf*) higher than 0.85 (lagging or leading) when the output is bigger than 10% of rating.

Table 1 Distortion limits as recommended in IEEE Std. 519-1992.

Odd	Limit (%)	Even	Limit (%)
$3^{rd} - 9^{th}$	< 4.0	2^{nd} - 8^{th}	< 1.0
11^{th} - 15^{th}	< 2.0	12^{th} - 16^{th}	< 0.5
17^{th} - 21^{st}	< 1.5	18^{th} - 22^{nd}	< 0.375
23^{rd} - 33^{rd}	< 0.6	24^{th} - 34^{th}	< 0.15
> 33^{rd}	< 0.3	> 34^{th}	< 0.075

2) Response to abnormal utility conditions - The inverter should sense the abnormal voltage and respond with the trip time as shown in Table 2 at the different voltage conditions at the point of common coupling (PCC). The inverter should cease to energize the utility line within six cycles when the utility frequency is out of the range of 59.3 ~ 60.5 Hz.

Table 2 Response to abnormal voltages.

RMS voltage (at PCC)		Maximum trip time (cycle)
Practice	Experiment (220V base)	Practice
V<50%	V<110	6
50%≤V<88%	110≤V<194	120
88%≤V≤110%	194≤V≤242	Normal operation
110%<V<137%	242<V<301	120
137%≤V	301≤V	2

3) Islanding detection time - If the real power to load mismatches larger than 50% and the island-load power factor is less than 0.95 (lagging or leading), the islanding should be detected within 10 cycles or less. Otherwise with a quality factor (Q) of 2.5 or less, it should be done within 2 seconds.

3. AFDPCF

As a method of overcoming the weaknesses of AFD, a novel AFD scheme, in which pulsation of chopping fraction deviates from the frequency in an instant away from nominal, is proposed. This scheme is referred to as AFD with pulsation of chopping fraction (AFDPCF). It can be modeled as below:

$$cf = \begin{cases} cf_{max} & \text{if } T_{cf\,max\_on} \\ cf_{min} & \text{if } T_{cf\,min\_on} \\ 0 & \text{otherwise} \end{cases} \quad (3)$$

where cf_{max} and cf_{min} are the maximum and minimum values of cf respectively. Figure 2 depicts the proposed method. The critical gains of the AFDPCF anti-islanding algorithm are values of cf and its on-time T_{cf_on}. In order to determine the values of cf, it is necessary to investigate the relationship between cf and current THD_i as shown in Fig. 3. The allowable limit of THD_i (5%) by the standard [1] sets an upper/lower limit on the usable value of cf (i.e. cf_{max} = 0.046, THD_i = 4.88% and cf_{mim} = -0.045, THD_i = 4.92%). Therefore, THD_i of the proposed method is always between 0.9% and 4.92%.

A systematic approach of NDZ of under/over voltage and under/over frequency was described in [6]. Normally, there are power mismatch quantities into the grid (i.e. $\Delta P \neq 0$, $\Delta Q \neq 0$) in a non-islanding situation as shown in Fig. 4. The voltage and frequency at the point of common coupling (PCC) will be changed by power mismatch conditions (ΔP, ΔQ) after islanding occurrence. The relationship between the power mismatch quantities and voltage/frequency thresholds can be derived as below:

$$\left(\frac{V}{V_{max}}\right)^2 - 1 \le \frac{\Delta P}{P} \le \left(\frac{V}{V_{min}}\right)^2 - 1 \quad (4)$$

$$Q_f\left(1-\left(\frac{f}{f_{min}}\right)^2\right) \le \frac{\Delta Q}{P} \le Q_f\left(1-\left(\frac{f}{f_{max}}\right)^2\right) \quad (5)$$

According to IEEE Std. 929-2000, V_{max} = 110%, V_{min} = 88%, f_{max} = 60.5Hz, f_{min} = 59.3Hz, Q_f = 2.5. Therefore, Eq. (4) and (5) can be derived as the followings:

$$-17.36\% \le \frac{\Delta P}{P} \le 29.13\% \quad (6)$$

$$-5.94\% \le \frac{\Delta Q}{P} \le 4.11\% \quad (7)$$

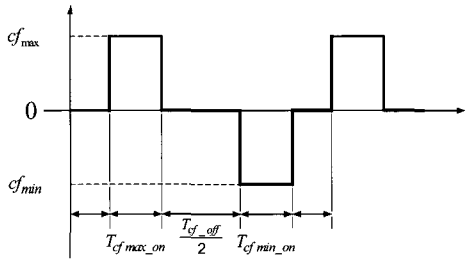

Fig. 2 Pulsation of chopping fraction cf.

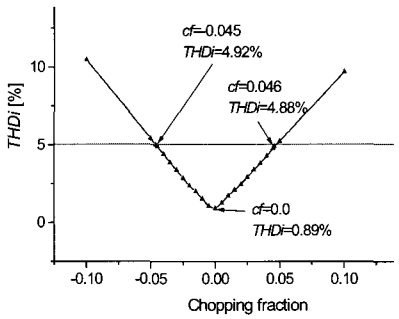

Fig. 3 Relationship of the THD_i vs. chopping fraction for the waveform in Fig. 1.

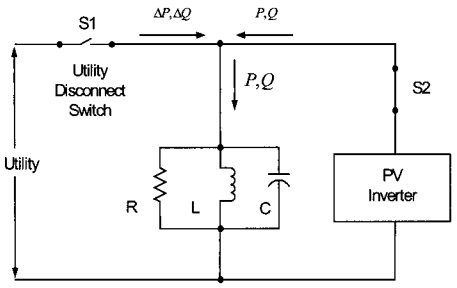

Fig. 4 Islanding test circuit after the grid is disconnected.

If the displacement power factor (*DPF*) is one unit, the power factor (*PF*) and the reactive power can be expressed as followed:

$$PF = \frac{P}{S} = \frac{1}{\sqrt{1+THD_i^2}} \tag{8}$$

$$\frac{Q}{P} = THD_i \tag{9}$$

Since the proposed method perturbs only the THD_i, it is assumed that $\Delta P/P$ is nearly zero. If $\Delta Q/P$ is nearly zero at the moment of islanding situation, the reactive power mismatch by *cf* is

$$\frac{\Delta Q_{cf\ max\_on}}{P} = 4.88\% \quad \text{at} \frac{\Delta Q}{P} \approx 0\% . \tag{10}$$

Therefore, it is out of the range in Eq. (7) and AFDPCF can detect the islanding instantly by over frequency relay (OFR) by Eq. (10). However, if $\Delta Q/P$ is nearly around the low limit (i.e. $\Delta Q/P \approx$ -5.94%) at the moment of islanding situation, the reactive power mismatch by *cf* is

$$\frac{\Delta Q_{cf\ max\_on}}{P} = -1.06\% \quad \text{at} \frac{\Delta Q}{P} \approx -5.94\% . \tag{11}$$

This means that the positive pulsation of chopping fraction, which increases the frequency, is not sufficient to detect the islanding entirety. Consequently, the negative pulsation of chopping fraction is required to decrease the frequency.

$$\frac{\Delta Q_{cf\ min\_on}}{P} = -10.86\% \quad \text{at} \frac{\Delta Q}{P} \approx -5.94\% \tag{12}$$

Therefore, it is out of the range in Eq. (7) and AFDPV can detect the islanding instantly by under frequency relay (UFR). In the zero value of power mismatching ($\Delta Q/P \approx 0$) situation, the transient time (T_{trans}) is required to reach the detectable frequency limits. According to the experimental results, it takes about 7 cycles to increase or decrease the frequency to the limit. However, 14 cycles is appropriate for securing system relativity. Therefore, the least period of T_{cfmax_on} and T_{cfmin_on} can be determined as

$$\begin{aligned} T_{cf\,\max\_on} = T_{cf\,\min\_on} &= T_{trans} + T_{trip} \\ &= 14 + 6 = 20[\text{cycle}] \end{aligned} \tag{13}$$

where T_{trip} is the maximum trip time (6 cycles) recommended by the standard [1]. Since islanding can be detected within 2 seconds in any scenario, the period of pulsation T_{cf} was determined to be 100 cycles in this paper. Finally, the period of T_{cf_off} is derived as

$$T_{cf\_off} = T_{cf} - (T_{cf\,\max\_on} + T_{cf\,\min\_on}) = 60 \text{ [cycle]}. \tag{14}$$

From Eqs. (7) and (12), the behavior of the proposed method is classified with the next three cases shown in Fig. 5. According to the standard [1], the range of ΔQ/P was limited to ±5%.

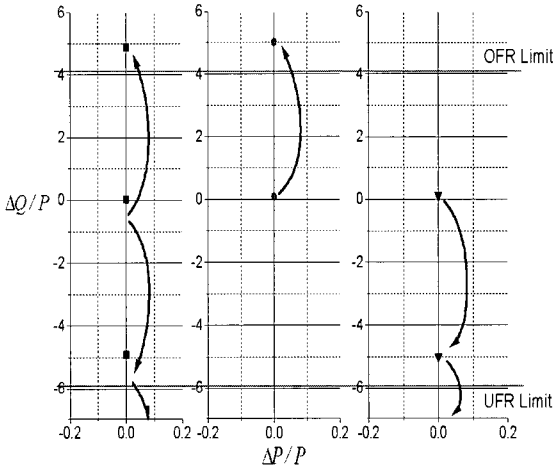

Fig. 5 behavior of the proposed method (AFDPV) in mapping of NDZ with different load conditions.

1) Case (a): $\Delta Q/P$ is nearly 0.0% at the islanding.

The frequency of the *PCC* voltage is nearly 60.0Hz at the moment of islanding occurrence. At that point, the frequency moves to 60.59Hz by injected positive *cf*. The OFR trips the system within T_{trip} (6 cycles). Otherwise, the frequency moves to 59.45Hz by the injection of the

negative *cf* and then the frequency drift down to the UFR limit within T_{cfmin_on}. The islanding can be detected within 50 cycles at least.

2) Case (b): $\Delta Q/P$ is nearly 5.0% at the islanding.

The frequency of the *PCC* voltage is approximately 60.61Hz at the moment of islanding occurrence. Since this value is over the OFR limit, the islanding can be detected within T_{trip} (6 cycles). However, if the negative *cf* is injected at the moment of islanding occurrence, the frequency moves to 60.04Hz. The frequency then moves to 60.61Hz by turning off the negative *cf*. Therefore, the islanding can be detected within 70 cycles at the least.

3) Case (c): $\Delta Q/P$ is nearly -5.0% at the islanding.

The frequency of the *PCC* voltage is approximately 59.4Hz at the moment of islanding occurrence. The frequency then moves to the UFR limit within the injected negative *cf*. Similar with case (b), if there is injected positive *cf* at the moment of islanding occurrence, the frequency moves to 60.01Hz. The frequency then moves to 59.4Hz by turning off the positive *cf*. After that time, the frequency moves to UFR limit within T_{cfmin_on} by the injection of negative *cf*. The islanding can be detected within at least the 70 cycles.

4. Experimental Results

To verify the validation of the proposed method, the islanding test results corresponding with IEEE Std. 929-2000 for a 3kW prototype inverter are presented. Specifically, to maintain the unity displacement power factor and drift the frequency in real time after the islanding, the real time continuous tracking phase locked loop (PLL) with digital all-pass filter is used [7,8].

Figure 6 shows the voltage and current waveforms of inverter output before and after the frequency drift. From Fig. 6(a), it is shown that the displacement power factor is regulated in unity. The harmonic spectra of the inverter output current at rated inverter output power 3kW are shown in Fig. 7 in cases at different *cf* values of 0, 0.046 and –0.045 respectively. The THD_i are respectively 0.9% and 4.92%, which are less than the limit of IEEE Std., 5%, and every individual harmonic below the limits of that standard in any case in Table 1. From the above, it is well verified that the proposed ADF method meets the power quality limit of IEEE Std.

The islanding test procedure of IEEE Std. 929-2000 indicates that the effective power mismatch (ΔP) and the reactive power mismatch (ΔQ) respectively have to be nearly zero with a quality factor (Q_f) of 2.5. After the islanding test, one parameter that is adjusted may be load inductance L where load capacitance *C* is adjusted within a total range ±5%.

In this paper, the experimental condition set as follow

$$P_{inv} = 3\,\text{kW}$$
$$P_{qL} = P_{qC} = Q_f \cdot P_{inv} = 2.5 \times 3 = 7.5\,\text{kVar}$$
$$\Delta P/P = 0$$
$$\frac{\Delta Q}{P} = 0,\ 150\text{var},\ -150\text{var}$$

Figure 8 shows the islanding test results under different load conditions. From Fig. 8, it is shown that the magnitude of the PCC voltage is not changed after islanding occurrence because $\Delta P/P$ is nearly zero. From Fig. 8(a), it is shown that the frequency increases up to 60.84Hz during T_{cfmax_on}. Since the transient time T_{trans} is 6 cycles and the maximum trip time T_{trip} is 5cycles, the islanding detection time is 11 cycles (0.183s). Figure 8(b) shows the test result under the same load condition as Fig. 8(a) ($\Delta Q/P \approx 0.0\%$), and islanding is detected by UFR. After islanding occurrence, the frequency maintains 60Hz during T_{cf_off} (30cycles). After that time, the frequency drifts down until 59.2Hz during T_{cfmin_on}. Figure 8(c) is the test result with load condition ($\Delta Q/P \approx 5.0\%$). After islanding, the frequency maintains 60.4Hz during T_{cf_off} (26cycles) and then the frequency drifts to 59.53Hz by the injection of the negative *cf* during T_{cfmin_on} (20cycles). After that time, the frequency increases up to OFR limit during T_{cf_off} (22cycles). It is noticed that the frequency increase is accomplished with the load condition ($\Delta Q/P \approx 5.0\%$) according to Eq. (7). Figure 8(d) is the test result with load condition ($\Delta Q/P \approx -5.0\%$). After islanding, the frequency maintains 59.6Hz during T_{cf_off} (4cycles) and then the frequency drifts up to 60.3Hz by the injection of the positive *cf* n during T_{cfmax_on} (20cycles) and then the frequency decreases to 59.3Hz during T_{cf_off} (30cycles). After that time, the frequency drifts down

rapidly by the injection of the negative *cf* during T_{cfmin_on} (3cycles).

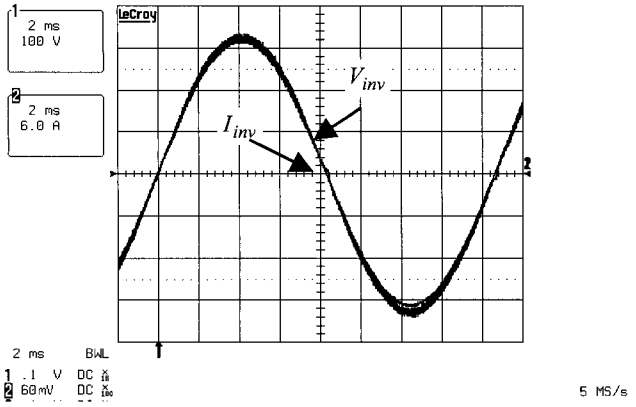

(a)

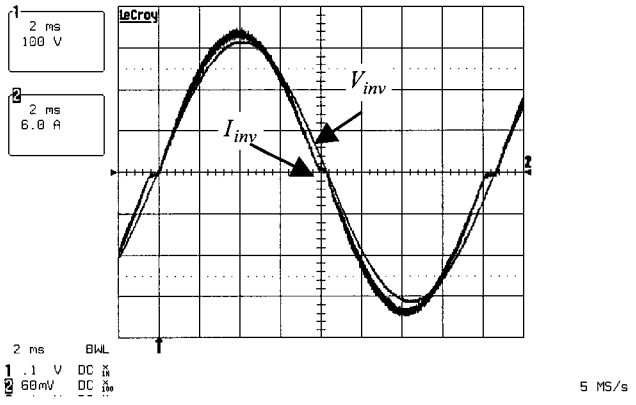

(b)

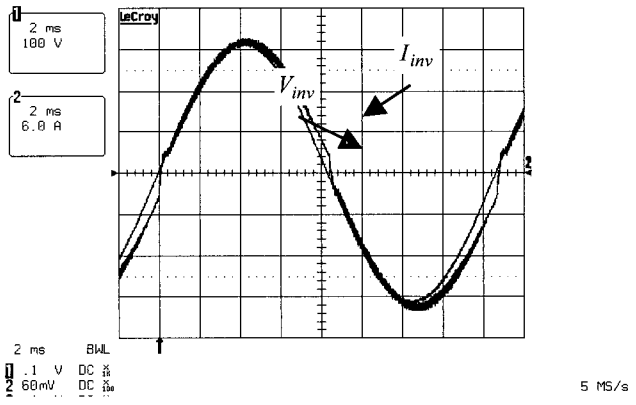

(c)

Fig. 6 Output voltage and current waveforms of the 3kW prototype PV system: (a) T_{cf_off} (*cf*=0.0), (b) T_{cfmax_on} (*cf*=0.046), (c) T_{cminf_on} (*cf*=-0.045) (CH 1: inverter voltage (V_{inv}) 100V/div, CH 2: inverter current (I_{inv}) 6A/div).

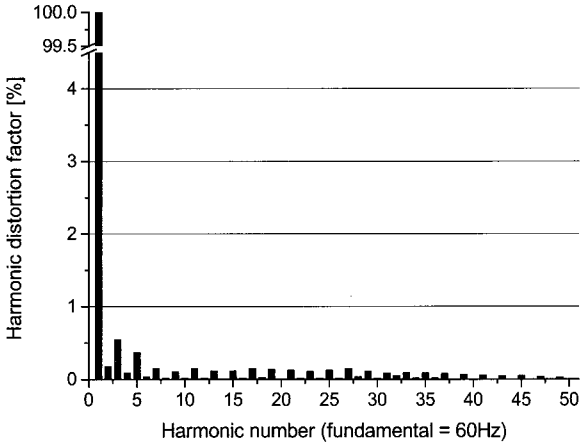

(a)

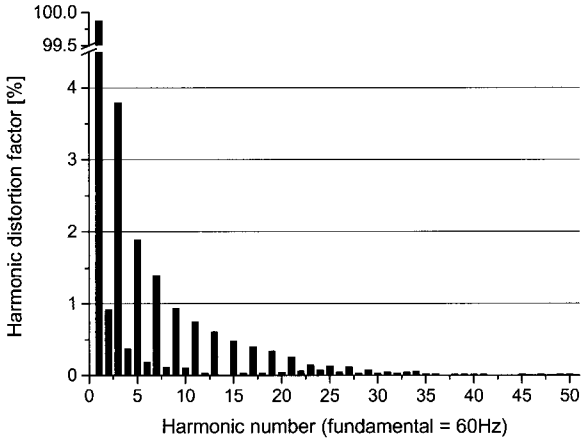

(b)

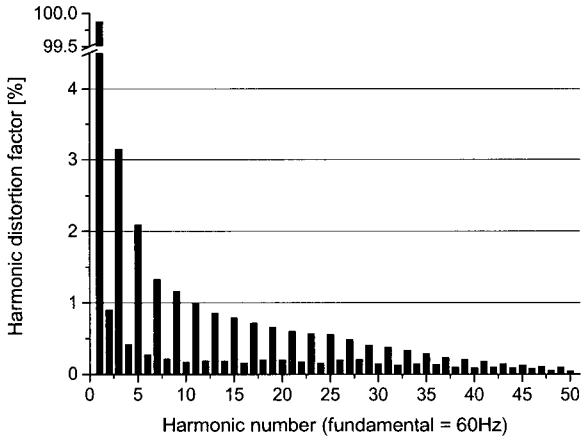

(c)

Fig. 7 Individual harmonic distortion factor of inverter output current: (a) T_{cf_off} (*cf*=0.0), (b) T_{cfmax_on} (*cf*=0.046), (c) T_{cfmin_on} (*cf*=-0.045).

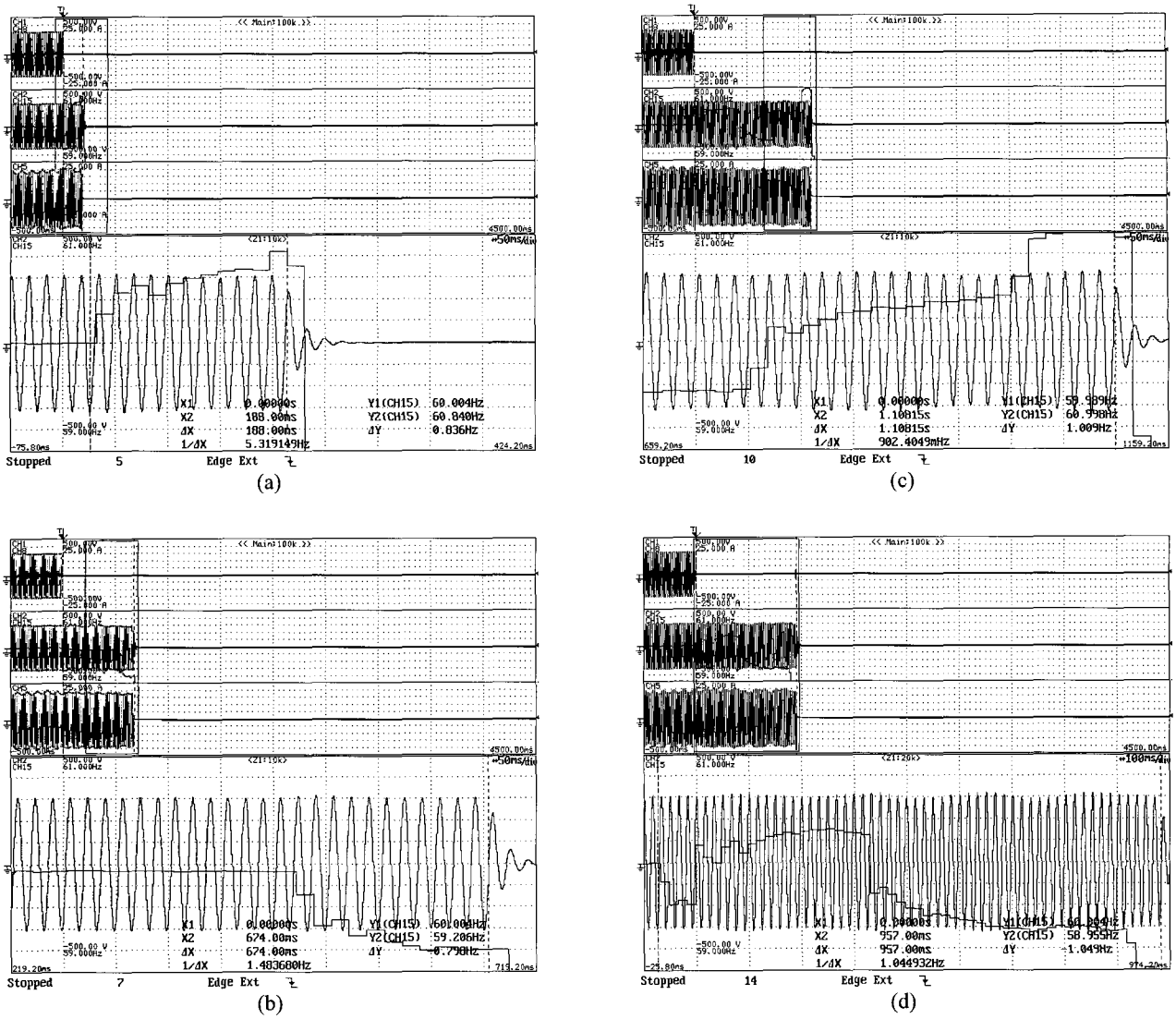

Fig. 8 Islanding test result with $\Delta P/P \approx 0.0\%$ and (a), (b) $\Delta Q/P \approx 0.0\%$, (c) $\Delta Q/P \approx 5.0\%$ (150var), (d) $\Delta Q/P \approx -5.0\%$ (-150var) (CH1: grid voltage 100V/div; CH8: grid current 5A/div; CH2: PCC voltage 100V/div; CH 15 frequency of PCC voltage 0.2Hz/div; CH5: inverter current 5A/div).

According the experimental results, islanding detection time is within 2 seconds for all the cases. The experimental results exactly correspond with the previous analysis. The islanding detection time with different load conditions was presented in Table 3.

Table 3 Islanding detection time with different load conditions.

ΔQ/P	0.0%	5.0%	-5.0%
Islanding detection time	0.674s	1.108s	0.957s

5. Conclusions

This paper presents the AFD with Pulsation Chopping Fraction (AFDPCF) method to improve the performance of conventional AFD methods. The experimental results of the AFDPCF show higher performance of islanding detection within 2 seconds and meet the power quality limit of IEEE Std. It is supposed that the inverter output current harmonic THD_i without cf are below 0.9%. However, to achieve this low THD_i, the system requires higher cost and considerable effort. Therefore, this paper proposes the mean THD_i concept, which is measured by

averaging the THD_i during several periods. The proposed system's $THD_{i,mean}$ is 2.8% over 2 seconds.

References

[1] IEEE Std. 929-2000, *IEEE Recommended Practice for Utility Interface of Photovoltaic (PV) Systems*, April, 2000.

[2] Jun Yin, Liuchen Chang, and Diduch, C., "Recent developments in islanding detection for distributed power generation," *2004 Large Engineering systems Conference of Power Engineering*, pp. 124-128, July 2004.

[3] G.A. Kern, "SunSine300, utility interactive AC module anti-islanding test results," *IEEE Photovoltaic Specialists Conference*, pp.1265-1268, Sept. 1997.

[4] M.E. Ropp, M. Begovic, and A. Rohatgi, "Analysis and performance assessment of the active frequency drift method of islanding prevention," *IEEE Trans. on Energy Conversion*, vol. 14, no. 3, pp. 810-816, Sept. 1999.

[5] V. John, Z. Ye, and A. Kolwalkar, "Investigation of anti-islanding protection of power converter based distributed generators using frequency domain analysis," *IEEE Trans. on Power Electronics*, vol. 19, no. 5, pp. 1177-1183, Sept. 2004.

[6] Z. Ye, A. Kolwalkar, Z. Yu, P. Du, and R. Walling, "Evaluation of anti-islanding schemes based on nondetection zone concept," *IEEE Trans. Power Electronics*, vol. 19, no. 5, pp. 1171-1176, Sept. 2004.

[7] Y. Jung, J. So, G. Yu, and J. Choi, "Modeling and analysis of active islanding detection methods for photovoltaic power conditioning systems," *2004 Canadian Conference of Electrical and Computer Engineering*, vol. 2, pp. 979-982, May 2004.

[8] H.S. Heo, H.S. Kim, H.G. Kim, G.H. Choe, Y.H. Choi, and J.C. Kim, "The Analysis and design of AFD Method for Anti-Islanding of single-phase UIPV System," *2006 Autumn Conference of Korean Institute of Power Electronics*, pp. 127~130, Nov. 2006.

[9] Y. Jung, J. Choi B. Yu, J. So, and G. Yu, "A Novel Active Frequency Drift Method of Islanding Prevention for the grid-connected Photovoltaic Inverter," *2005 IEEE 36th Conference on Power Electronics Specialists*, pp. 1915-1921, Sept. 2005.

Youngseok Jung received his B.S., M.S., and Ph.D. degrees from the Chungbuk National University in Cheongju, Korea in 1994, 1996, and 2006, respectively. He has been with the Photovoltaic Research Group at Korea Institute of Energy Research since 1996, where he is currently a senior researcher. His research areas include power electronics, grid-connected inverter, test and evaluation of photovoltaic system.
He is an active member of KIEE, KIPE, IEEE.

Jaeho Choi received his B.S., M.S., and Ph. D. degrees in electrical engineering from the Seoul National University in Seoul, Korea in 1979, 1981, and 1989, respectively. From 1981 to 1983, he worked as a full-time lecturer in the Department of Electronic Engineering at the Jungkyoung Technical College in Daejeon. He has been with the School of Electrical and Computer Engineering at Chungbuk National University in Cheongju, Korea since 1983, where he is currently a professor. In 1993, 1998, and from 2003 to 2004, he was a visiting professor at the University of Toronto in Toronto, Canada. He was a Danfoss visiting professor of Aalborg University, Denmark, in 2002. His research areas include power electronics, power quality problems and solutions, static power converter, UPS, and energy storage systems, and electric traction drives. He is an active member of KIEE, KIPE, and IEEE, and currently the vice president of KIPE and the editor-in-chief of JPE.

Gwonjong Yu received the B.S. degrees in the Electrical Engineering from the Chosun University, Gwangju, Korea, in 1982, and the M.S. and Ph. D. degree in the Electrical engineering from Kobe University, Kobe, Japan, in 1985 and 1989, respectively.
He has been with the Photovoltaic Research Group at Korea Institute of Energy Research, Daejeon, Korea since 1990, where he is currently a group leader. His research areas include power electronics, Photovoltaic system and PV module, and energy storage systems.
He is an active member of KIEE, KIPE, IEEE,.